A theoretical study of the crystallographic structures in neptunium

1994 J. Phys.: Condens. Matter 6 6573

(http://iopscience.iop.org/0953-8984/6/33/006)

J. Phys.: Condens. Matter 6 (1994) 6573–6580. Printed in the UK

A theoretical study of the crystallographic structures in neptunium

P Söderlind†, J M Wills‡, A M Boring‡, B Johansson† and Olle Eriksson†

† Condensed Matter Theory Group, Department of Physics, University of Uppsala, Box 530, Uppsala, Sweden

‡ Center for Materials Science and Theoretical Division, Los Alamos National Laboratory, Los Alamos, NM 87545, USA

Received 21 April 1994

Abstract. The total energy has been calculated as a function of volume for various crystal structures in neptunium metal. Around the equilibrium volume the experimentally observed low-temperature structure, α-Np, is found to have the lowest energy. As a function of compression we predict Np to undergo a crystallographic phase transition from α-Np to BCC. The zero-temperature calculations also show that at volumes close to the α-Np $\rightarrow$ BCC transition the BCT structure is very close in energy, and high-pressure experiments performed at elevated temperatures on Np may allow observation of this structure as well.

1. Introduction

The light actinides (Ac–Pu) have certain physical properties that resemble the transition metals, e.g., the volumes decrease parabolically as the series is traversed. This is now understood to be caused by the gradual filling of the itinerant 5f band, quite similar to the filling of the d band in the transition metals. However, there are pronounced differences between the actinides and the transition metals. The latter have FCC, HCP, or BCC crystal structures, whereas the light actinides show much more complicated structures at low temperatures: Th (FCC), Pa (BCT), U (orthorhombic, two atoms/cell), Np (orthorhombic, eight atoms/cell) and Pu (monoclinic, 16 atoms/cell). Also, the melting temperatures are anomalous, [1] as are the thermal expansion coefficients [2]. The behaviour of the bulk modulus as well as the behaviour of the cohesive energy for the light actinides is also quite different from the trend exhibited by the transition metals [1]. The trend in the cohesive energy was demonstrated by Brooks [3, 4] to be caused by an interplay between the band energy contribution of the solid and the spin polarization energy of the atom. In an earlier communication we demonstrated that the low-symmetry structures encountered in Pa and U are consistent with itinerant f electrons, and it was shown that for Th, Pa, and U the calculated energy (when comparing the FCC, BCT, and α-U structure) is lowest for the experimentally observed structure [5], i.e., FCC for Th, BCT for Pa, and α-U for U. It has also been demonstrated that Th, under pressure, undergoes an FCC $\rightarrow$ BCT phase transition which is connected to an increased f occupation as a function of increasing pressure [6, 7].

Hence it seems that itinerant f electrons drive low-symmetry structures, and in this context it is interesting to observe that Np and Pu, at low temperatures, also exhibit low-symmetry structures. As mentioned above, at low temperatures Np crystallizes in the orthorhombic α phase, with eight atoms/cell [8]. A small increase in temperature

0953-8984/94/336573+08$19.50

stabilizes the β-phase (278–540 °C), which is tetragonal with four atoms/cell [9]. These two structures can be viewed as heavy distortions of the BCC structure (which is found in Np in the temperature range 540–640 °C). The structures of α- and β-Np are, as pointed out by Zachariasen [8,9], very similar. To illustrate this we list in tables 1 and 2 the crystallographic parameters of these two structures.

Table 1. Lattice constants for α-Np [6] and β-Np [9].

	a (Å^3)	b (Å^3)	c (Å^3)
α-Np	4.723	4.887	6.663
β-Np	4.897	—	3.388

Table 2. Atomic positions for α-Np [6] and β-Np [9].

Atom type	Atomic positions	
α-Np(I)	$\pm(\frac{1}{4}, y_1{}^a, z_1{}^b)$	$\pm(\frac{1}{4}, \frac{1}{2} - y_1, z_1 + \frac{1}{2})$
α-Np(II)	$\pm(\frac{1}{4}, y_2{}^c, z_2{}^d)$	$\pm(\frac{1}{4}, \frac{1}{2} - y_2, z_2 + \frac{1}{2})$
β-Np(I)	(0, 0, 0)	$(\frac{1}{2}, \frac{1}{2}, 0)$
β-Np(II)	$(\frac{1}{2}, 0, u^e)$	$(0, \frac{1}{2}, -u)$

[a] $y_1 = 0.208$.
[b] $z_1 = 0.036$.
[c] $y_2 = 0.842$.
[d] $z_2 = 0.319$.
[e] $u = 0.375$.

In a recent report [10], it was shown that when the 5f bandwidth of Th and U becomes comparable to the d bandwidth of the transition metals, both Th and U stabilize first in the BCT structure and then in the BCC structure. In this work it was demonstrated that at zero temperature the crystallographic arrangement of the actinide elements is determined by the same interactions and effects that stabilize the structures of the transition metals. In particular the Peierls distortion/Jahn–Teller effect was demonstrated to be dominant at larger volumes (where the 5f band is narrow), dictating open structures, whereas at higher compression (when the 5f band is of comparable width to d bands for the transition metals) the Madelung energy stabilizes close packed structures (e.g. BCC).

We have been motivated to conduct a similar investigation concerning the crystallographic phases of Np as a function of compression. If the arguments presented by Söderlind *et al* [10] are valid one would expect to see crystallographic phase transitions to more symmetric and close-packed structures in Np also as a function of compression. Experimental studies of Np under high compressions have not been reported and we hope that the present theoretical work can stimulate experimental efforts. Also, it is of interest to investigate whether a theory based on the local approximation to density functional theory can reproduce the extremely complicated crystal structures found in Np. We have thus compared the total energies of the α-, β-, BCT, BCC, and FCC structures of Np as a function of volume.

The rest of this paper is organized as follows: in section 2 we describe the details of our calculations, in section 3 we report our results, and in section 4 we present our conclusions.

2. Details of the calculation

The computational details of this work are very similar to those of our previous studies on crystal structures of f electron materials [5, 11]. We have used a full potential linear muffin tin orbital technique [12, 13]. Exchange and correlation were treated in the local density approximation using the Hedin–Lundqvist exchange–correlation functional. The calculations were all electron, fully relativistic (spin-orbit coupling included at each variational step [14]), and employed no shape approximation to the charge density or potential. The basis set, charge density, and potential were expanded in spherical harmonic series within non-overlapping muffin tin spheres and in Fourier series in the interstitial region between the spheres. The volume of the muffin tin spheres was set at a fixed fraction (approximately 0.50) of the total volume, for all structures and volumes.

The basis set, comprised of augmented linear muffin tin orbitals [14, 15], contained 6s, 6p, 7s, 7p, 6d, and 5f partial waves in a single, fully hybridizing 'energy panel'. The inclusion of the 6s and 6p partial waves as band states rather than as core states was necessitated by the small size of the muffin tin spheres. Two sets of energy parameters [14, 15], one with energies appropriate to the 'pseudocore' 6s and 6p bands and one with energies corresponding to the valence bands were used to calculate the radial functions for the expansions of the bases in the muffin tins. Also, we used a so called double basis set, to ensure a well converged basis set. Approximate orthogonality between bases with the same ℓ value was maintained by energy separation.

Integration over the Brillouin zone (BZ) was done using 'special point' sampling [16]. The results reported here used 60 points (FCC), 27 points (β-Np), 16 points (α-Np), 80 points (BCT), and 59 points (BCC) in the irreducible wedge of the BZ. Increasing the number of k-points modified the energy difference between the different structures with a fraction of one mRyd.

3. Results

Before comparing the calculated energies of the different crystal structures we optimized the crystallographic parameter of the BCT structure. This was necessary since no experimental data are available for this structure in Np (for the α and β structures we used the experimental crystal data, see tables 1 and 2). Thus we show in figure 1 the calculated energy of BCT Np as a function of the c/a ratio. The calculation presented in figure 1 was performed for a fixed volume, which was kept equal to the experimental volume of Np. The lowest energy is found at $c/a = 0.85$ and throughout the rest of the calculations (to be presented below) we used this c/a ratio for the BCT structure. Notice from figure 1 that there is a second minimum at $c/a \approx 1.8$. The two minima in figure 1 are close to what is experimentally observed in Pa (0.825) and Th under pressure (1.65). Notice also that at $c/a = 1$ (equal to the BCC structure) there is no local minimum in the total energy. This suggests that BCC Np, at low temperatures, is unstable towards a tetragonal distortion. A recent calculation [17] giving negative elastic constants for BCC Np indeed confirms this picture. Nevertheless, at elevated temperatures (540 °C) the BCC structure is stabilized in Np.

The calculated total energies of α-, β-, BCT, FCC, and BCC Np as a function of volume are shown in figure 2. The FCC structure energy is higher than the BCC structure energy for the studied volume interval, in good agreement with calculations by Skriver [18]. From figure 2 it is clear that the low-temperature structure, α-Np, is found to be the most stable crystal structure at the equilibrium volume. The present calculations thus reproduce the

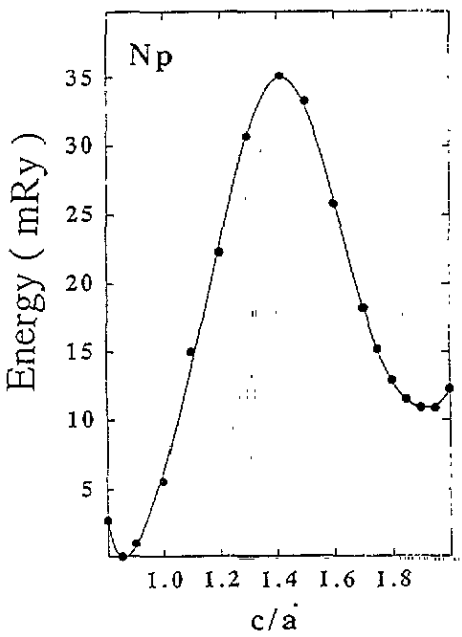

Figure 1. The calculated energy for BCT Np as a function of the c/a ratio.

correct ground state for Np. Notice also that the calculated equilibrium volume (16.6 Å^3) is in acceptable agreement with the experimental low-temperature value (19.2 Å^3). From the curvature of the total energy curve (at the experimental equilibrium volume) we compute the bulk modulus to be 1.7 Mbar, which should be compared to the experimental bulk modulus of 0.74 Mbar. The present calculation thus underestimates the equilibrium volume and overestimates the bulk modulus, which is a common feature for LDA calculations.

From figure 2 we notice that at compressed volumes we predict that the BCC structure becomes stable. From this figure it is also clear that at volumes close to the phase transition the BCT structure is only marginally higher in energy than the structure with lowest energy. It is thus possible that high-pressure experiments conducted on Np would detect a BCT structure as well. It should be remembered that the calculations presented in figure 2 are at zero temperature and that experiments performed at elevated temperatures are likely to yield somewhat different results transition pressures and volumes, and possibly they may also find the BCT structure stable over a small volume interval. However, moderate temperatures are not believed to change the gross features shown in figure 2 and we predict that at sufficiently small volumes Np stabilizes in the BCC structure. The pressure needed to obtain the BCC phase is well within experimental reach. The only experimental result available for a comparison with the results presented in figure 2 is the finding that the stabilization temperature of the BCC structure in Np initially decreases with pressure and if this phase boundary is extrapolated to zero temperature the BCC structure becomes stable at sufficiently large pressures. Due to the extreme uncertainty of such an extrapolation we have refrained from estimating a zero-temperature transition pressure from the experimental data. Notice further in figure 2 that the FCC phase lies higher in energy than the other phases for the studied volumes, and thus this phase is not even close to being stable in Np at equilibrium or at applied pressure. It is also interesting to observe that the energy minimum calculated for the FCC phase is considerably larger than the equilibrium volume calculated

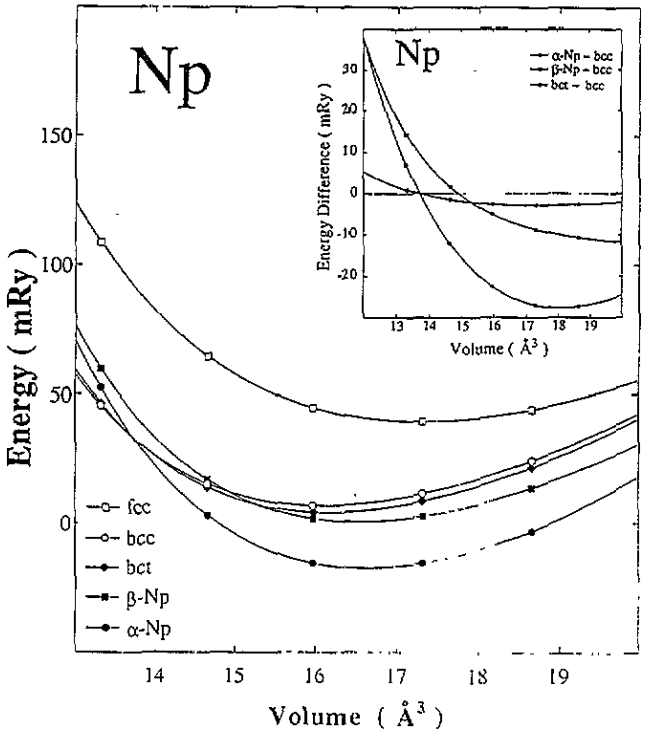

Figure 2. The calculated total energy for α-Np, β-Np, BCT Np, BCC Np, and FCC Np as a function of volume. The inset shows the energy difference between α-Np and BCC, β-Np and BCC, and also between BCT and BCC. Thus the BCC phase is here the zero level.

for the BCC phase, as well as the BCT, β, and α phases. In fact, the FCC equilibrium volume is closer to the experimental equilibrium volume than the other analysed phases, including α-Np. This finding, that calculations for FCC Np are in closer agreement with experiment than calculations for the correct (α) phase was also observed in a recent report [20].

In figure 3 we compare our calculated densities of states (DOSs), for α-Np (a) and β-Np (b). For each structure we have shown the 5f partial DOS from one of the atom types. Since the other atom types all have very similar local 5f DOSs we choose not to display them all. Notice that the valence band starts at $\sim$ 0.3 Ryd below the Fermi level (E_F), and that the DOS is dominated by the 5f contribution. It is also clear from this figure that the total 5f bandwidth is relatively broad. There are some differences between the DOSs of the two allotropes. For instance the β-phase has a sharp peak at 0.05 Ryd below E_F whereas in α-Np this peak is broader and found at slightly lower energies. Our calculated DOSs (figure 3) are actually quite similar to the DOS calculated earlier by Boring *et al* [19] and by Albers *et al* [21], who used a linear muffin tin orbital method in the atomic sphere approximation (ASA). It is interesting to note that our (full potential) results agree quite well with ASA results, even for quite open structures such as the β phase of Np.

In figure 4 we show the charge density contours of α-Np and in figure 5 those for β-Np. The charge density of α-Np was calculated in the y–z plane. There are no atoms lying in this plane; instead the atomic positions are at a quarter of the a lattice constant above or below the plane shown in figure 4 (see table 2). The anisotropy of the charge density and therefore the small covalent character of the chemical bonding is nevertheless obvious from

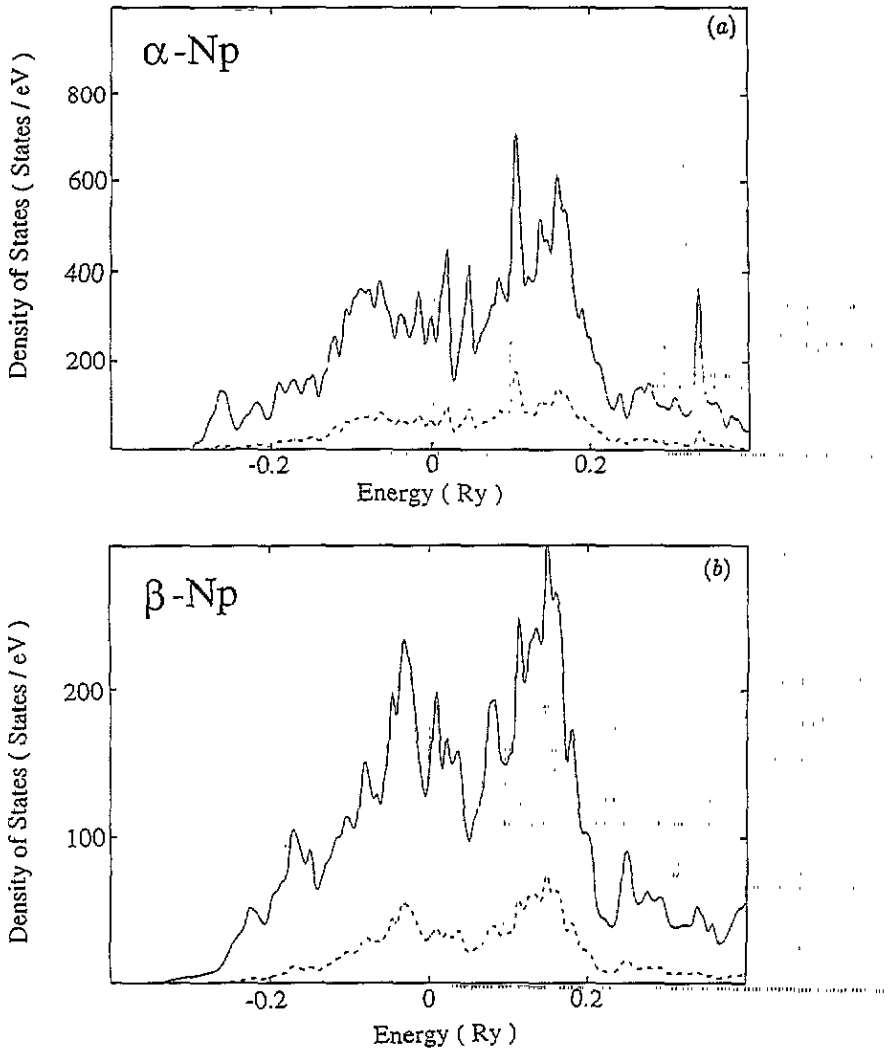

Figure 3. Calculated densities of states for α-Np (*a*) and β-Np (*b*). The solid line denotes the projection on the 5f states. The 6d density of states is marked with a dashed line.

this figure as it also in the β structure (shown for a cut in the x–z plane, figure 5). There is thus a good amount of charge piling up in between atoms in these two structures, an effect which is absent from the close-packed, symmetric structures (BCC, not shown). From figure 5 it is also clear that these structures are quite layered in the sense that there is a region in space where the density is very low.

4. Conclusions

To conclude we have, by means of first-principles calculations, reproduced the low-temperature structure of Np as well as obtaining a theoretical prediction of a crystallographic phase transition from α-Np to the BCC structure. Our findings are in agreement with the results of Söderlind *et al* [10], who demonstrated that the crystal structures of the f electron

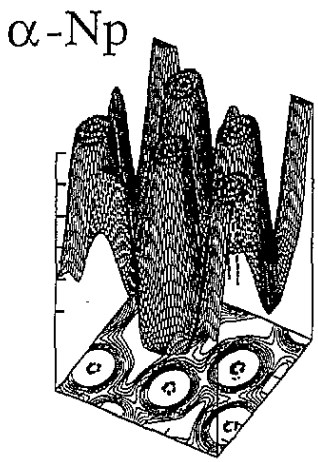

Figure 4. A charge density contour plot for α-Np.

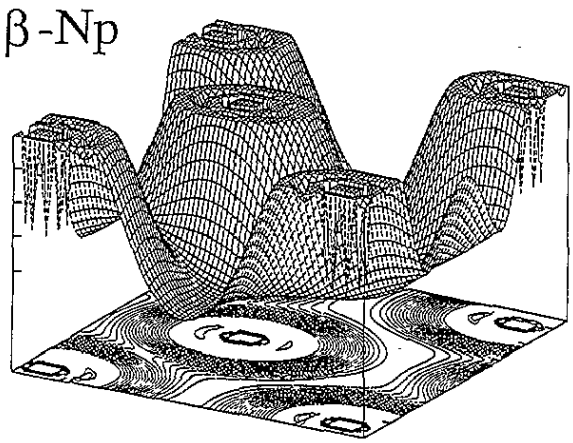

Figure 5. A charge density contour plot for β-Np.

elements can be understood as a competition between a Peierls distortion (favouring low-symmetry structures at high volumes) and the Madelung energy (favouring symmetric, close-packed structures at low volumes). The BCT structure is found to have only marginally larger energy compared to the low-energy structure at volumes close to the α-Np $\rightarrow$ BCC phase transition. It is therefore likely that high-pressure experiments on Np would also detect the BCT structure at sufficiently large compression. Finally we have demonstrated that the chemical bonding in α- and β-Np has some covalent character, since charge is found to pile up in between the atoms. It should be mentioned however that the bonding is mostly metallic in character, but it is interesting to note that these materials, which are good metals, also have a considerable covalent character in the chemical bonds.

Acknowledgments

Valuable discussions with B R Cooper and R C Albers are acknowledged. We are grateful to the Swedish National Supercomputer Centre (NSC) in Linköping where part of the calculations were performed.

References

[1] See articles in:
Freeman A J and Lander G H (ed) 1984 *Handbook on the Physics and Chemistry of the Actinides* (Amsterdam: North-Holland)
[2] A theoretical calculation and quoted experimental data can be found in
Söderlind P, Nordström L, Youngming L and Johansson B 1990 *Phys. Rev.* B **42** 4544
[3] Brooks M S S 1983 *J. Magn. Magn. Mater.* **29** 257; 1983 *J. Phys. F: Met. Phys.* **13** 103
[4] Brooks M S S, Johansson B and Skriver H L 1984 *Handbook on the Physics and Chemistry of the Actinides* ed A J Freeman and G H Lander (Amsterdam: North-Holland) ch 3, p 153
[5] Wills J M and Eriksson O 1992 *Phys. Rev.* B **45** 13 879
[6] Vohra Y K and Akella J 1991 *Phys. Rev. Lett.* **67** 3563
[7] Eriksson O, Söderlind P and Wills J M 1992 *Phys. Rev.* B **45** 12 588
[8] Zachariasen W H 1952 *Acta Crystallogr.* **5** 660
[9] Zachariasen W H 1952 *Acta Crystallogr.* **5** 664
[10] Söderlind P *et al* to be published
[11] Wills J M, Eriksson O and Boring A M 1991 *Phys. Rev. Lett.* **67** 2215
[12] Wills J M and Cooper B R 1987 *Phys. Rev.* B **36** 3809
[13] Price D L and Cooper B R 1989 *Phys. Rev.* B **39** 4945
[14] Andersen O K 1975 *Phys. Rev.* B **12** 3060
[15] Skriver H L 1984 *The LMTO Method* (Berlin: Springer)
[16] Chadi D J and Cohen M L 1973 *Phys. Rev.* B **8** 5747
Froyen S 1989 *Phys. Rev.* B **39** 3168
[17] Söderlind P, Eriksson O, Wills J M and Boring A M 1993 *Phys. Rev.* B **48** 9306
[18] Skriver H L *Phys. Rev.* B **31** 1909
[19] Boring A M, Schadlerv G, Albers R C and Weinberger P 1988 *J. Less Common Met.* **144** 71
[20] *Söderlind P et al Phys. Rev. B to be published*
[21] Albers R C *et al* to be published